

Histopathological changes result from exposure to *Staphylococcus aureus* enterotoxin b

Ahmed Farhan, Khadija Hamad*

Department of Biology, College of Science, University of Anbar, Al Ramadi, Iraq

*Email: biokhadija1996@gmail.com

Received: 02 October 2023 / Revised: 26 November 2023 / Accepted: 26 November 2023 / Published online: 28 November 2023.

How to cite: Farhan, A., Hamad, K. (2023). Histopathological changes result from exposure to *Staphylococcus aureus* enterotoxin b, *Journal of Wildlife and Biodiversity*, 7 (Special Issue), 730-745. DOI: <https://doi.org/10.5281/zenodo.10368039>

Abstract

Staphylococcal enterotoxin B (SEB), a potent inducer of toxic shock syndrome (TSS) and a potential biological threat agent, is known for causing classic food poisoning symptoms, such as fever, vomiting, and diarrhoea. Its superantigenic properties lead to extensive T-cell proliferation and the production of inflammatory cytokines, contributing to the severe effects of SEB. This toxin induces a wide range of histological changes in the liver, lung, and small intestine. This study involved thirty (20) albino rats obtained from the Iraqi Center for Cancer Research and Medical Genetics at Al-Mustansiriya University. These rats were treated with SEB via the intraperitoneal route (ip) and intragastric (ig), while five (5) female albino rats were used as a control. Histological slides revealed a broad spectrum of histopathological changes in the liver and lung caused by SEB toxin. SEB demonstrated the ability to activate a significant fraction of T lymphocytes, leading to a cytokine storm that resulted in substantial damage to internal tissues.

Keywords: Enterotoxin B(SEB), *Staphylococcus aureus*, histological changes

Introduction

Staphylococcal enterotoxin B (SEB), a potent superantigenic toxin and a recognized bioweapon, is generated by the main human infectious *S.aureus*. SEB, a 28-kDa protein with 239 amino acids, is closely related to SEC1, with a 67% amino acid composition similarity

and structural similarities (Murray,1998). SEB is heat labile, water soluble, and resistant to pepsin, trypsin, and papain as well as other proteolytic enzymes (MADIGAN et al,2004). The most powerful staphylococcal enterotoxin, and significantly less amounts are required to cause a harmful impact than with manufactured compounds. SEB is also very stable and simple to manufacture in big amount. SEB may result in multiple organ failure and death at low doses (Tortora et al,2004). Unlike conventional antigens, Superantigens have the ability to activate almost a fifth, or 20%, of the T-cell repertoire in the host. . They are able to avoid traditional antigen processing and presentation, which gives them an important advantage (Jardetzky et al,1994). effect of seb on liver In mice given SEB alone, hepatic necrosis was not seen, but Kupffer cells showed morphological changes, the most remarkable of which was an increase in size and number; in other study showed and moderate portal lymphoplasmacytic hepatitis (Finegold,1967). SEB administration increases aspartate aminotransferase (AST) levels, necrotic lesions, and the inflammatory storm (Zhang et al,2019). In lung tissue Exposure to staphylococcal enterotoxin B (SEB) might result in potentially fatal implications due to the activation of up to 40% of T and perhaps NKT cells (Marrack et al,1990; Marrack et al,1990), Inflammatory cytokines such IL-1, IL-2, IL-6, IFN, and TNF are produced as a result of this elevated response (Marrack et al,1990; McKallip et al,2002). This may result in vascular collapse (shock), acute lung injury (ALI), acute respiratory distress syndrome (ARDS), and damage to endothelial cells (Rajagopalan et al,2006). The development of SEB-induced ARDS/ALI was revealed to be significantly influenced by hyaluronic acid (Hayworth et al,2012). The study specifically found that SEB exposure raises hyaluronic acid levels in the lung, which suggests that hyaluronic acid production could be a viable target for the treatment or attenuation of SEB-induced lung damage (Schramm et al,2003).

Material and methods

Thirty (30) isolates of *S.aureus* were isolated from different clinical samples including (urinary tract infections, Eye swabs, wounds and cerebrospinal fluid (csf)), from Al-Fallujah teaching hospital. these isolates were identified depending on microscopic, cultural and biochemical tests and further identification by vitek2 compact.

Molecular identification of enterotoxin b gene (entb)

Extracted of Bacterial genomic DNA was directly from the 30 *S.aureus* clinical isolates using a special extraction kit using the Presto Mining DNA bacteria set from Geneaid company USA (No. GBB 101). This test used gene-specific primers to identify SEB genes (3-7) DNA amplification was performed in a final reaction mixture volume of 25 μ l (GoTaq® Green Master Mix, Promega, USA) with a total of thirty cycles(Zeinodini et al,2017). The toxin was purified according to (Schantz et al,1965).

Table 1. Primer sequences of *SEB* gene

Primer	Sequence	PCR product
SEB-F	GTTTCGGGTATTTGAAGATGG	226bp
SEB-R	CAAATTTATCTCCTGGTGCA	

Table 2. Uniplex PCR mixtures and conditions for identification of *SEB* gene

PCR mixtures		PCR conditions		
Contents	Volume	Type of cycle	Condition	No. of cycles
Master Mix	12.5 μ l	Initialization	94 °C for 5 min	1
Forward Primer	2.5 μ l	Denaturation	94 °C for 1 min	30
Reverse Primer	2.5 μ l	Annealing	60 °C for 1 min	
Template DNA	3 μ l	Extension	72 °C for 1 min	
Nuclase-Free Water	4.5 μ l	Final Extension	72 °C for 10 min	1

Experimental animals

In the animal house of the Iraqi Center for Cancer Research and Medical Genetics of AlMustansiriya University,20 (n = 20) female albino rats, aged 6-8 weeks, weighed (200–250)g. The rats were fed pellets and water when the room temperature was 22 ± 3 °C. Before the experiments, the rats were given two weeks for adaptation.these animals treated with SEB toxin via intraperitoneal(25 μ g) route and intragastric route(10 μ g) for seven days. Harvested lungs and liver were fixed in 10% formalin solution for two days then the tissue samples

were washed up by tap water before being embedded into paraffin and obtaining 5- μ m sections for haematoxylin and eosin (H&E) staining. H&E slides were imaged and analysed

Results

Agarose gel electrophoresis of PCR product obtained with enterotoxin B gene -specific primers that generated 226bp amplicon from *Staphylococcus aureus* strains (Fig. 1).

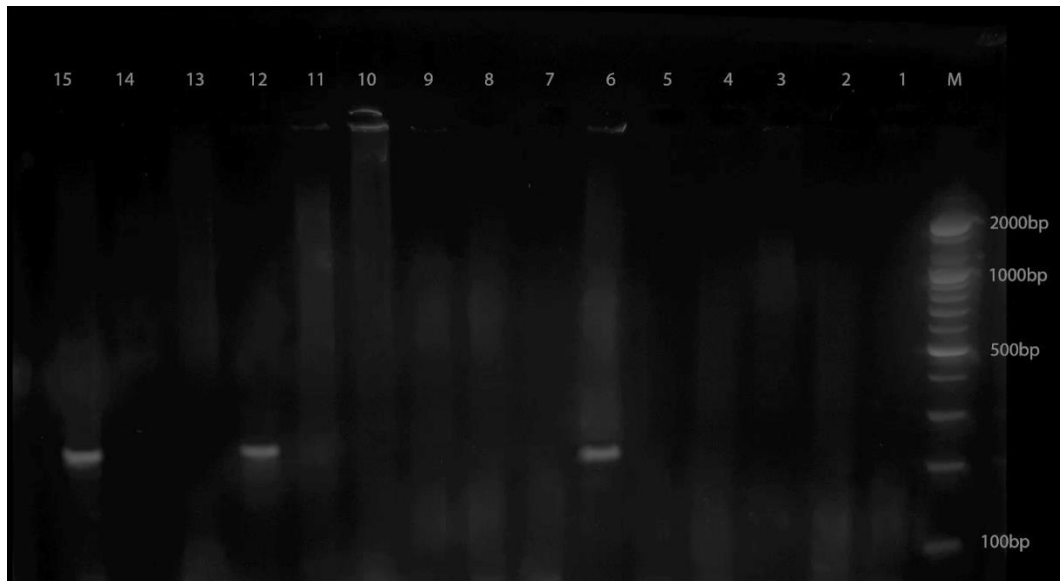


Figure 1. Agarose gel electrophoresis of PCR product obtained with *enterotoxin B gene* -specific primers that generated 226bp amplicon from *Staphylococcus aureus* strains. Lanes (1-15); represent the first 15 strains, and Lanes 6, 12 and 15 represent the positive isolates. Lane M represent 100bp DNA ladder

Histopathological changes in the liver

Histopathological figures of the liver of all animals revealed marked generalized cellular swelling with necrosis of hepatocytes (Fig. 2). The portal triad showed pre-vascular aggregation of MNLs with vascular dilation and congestion of the portal vein (Fig. 3). Other figures revealed hepatic steatosis (fatty changes) and necrosis of hepatocytes (Fig. 4), intravascular hemolysis with mild pre-vascular cuffing (aggregation of MNLs), and a portal triad with steatosis of hepatocytes (Fig. 5). Other figures of the liver revealed marked liver cirrhosis that was characterized by thickening of the interlobular connective tissue with marked sinusoidal dilation (Fig. 6). The magnified figure showed marked sinusoidal infiltration of lymphocytes and monocytes (Fig. 7). Other figures showed vascular

congestion, pre-vascular infiltration of MNCs at the portal triad, and moderate cellular swelling (Fig. 8).

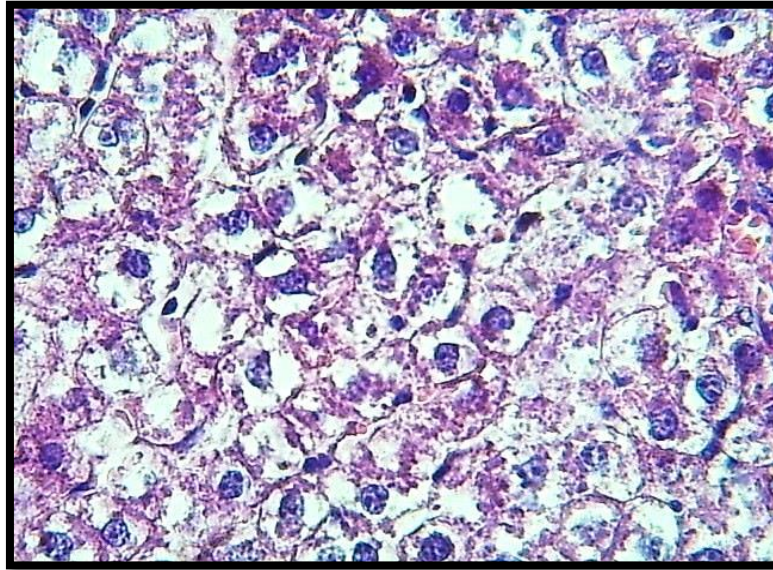


Figure 2. Marked cellular swelling with necrosis of hepatocytes. H&E stain 40x



Figure 3. shows pre-vascular aggregation of MNLs (black arrow) with vascular dilation and congestion of the portal vein (red arrows) and necrosis of hepatocytes (black arrows). H&E stain 100x

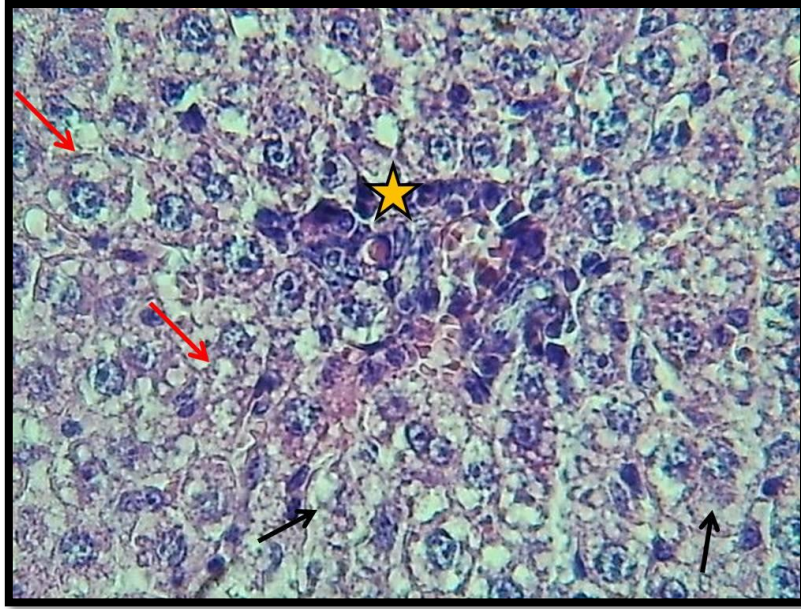


Figure 4. Section of liver (Group-B) shows: pre vascular aggregation of MNLs (Asterisk) with hepatic steatosis (Fatty changes) (Red arrows) and necrosis of hepatocytes (Black arrows) .H&E stain 400x.

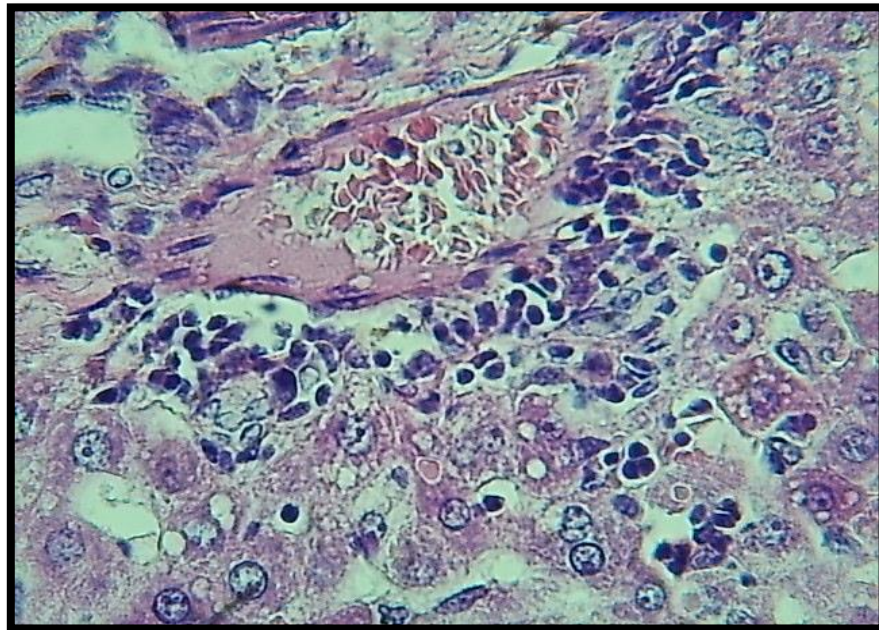


Figure 5. shows intra-vascular hemolysis with mild pre-vascular cuffing (aggregation of MNLs) and steatosis of hepatocytes. H&E stain 40x.

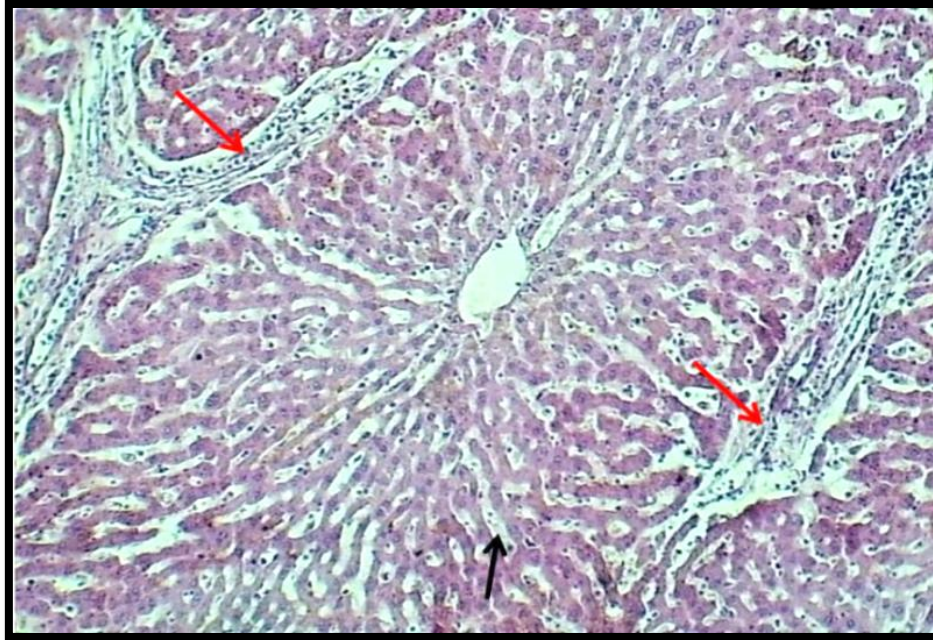


Figure 6. This figure shows marked liver cirrhosis characterized by thickening of interlobular connective tissue (red arrows) and marked sinusoidal dilation (black arrows). H&E stain 10x.

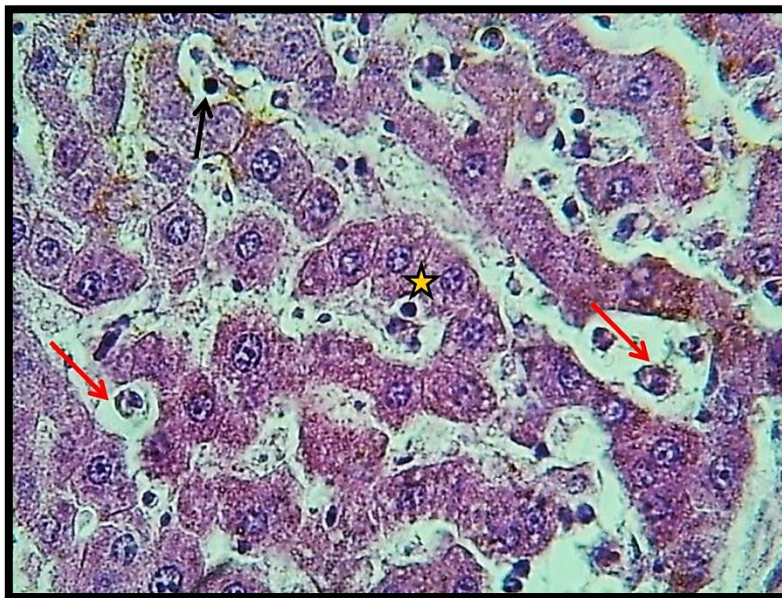


Figure 7. This figure shows a section of the liver (group E) with marked sinusoidal dilation with infiltration of lymphocytes (black arrow) and monocytes (red arrows). H&E stain 400x.

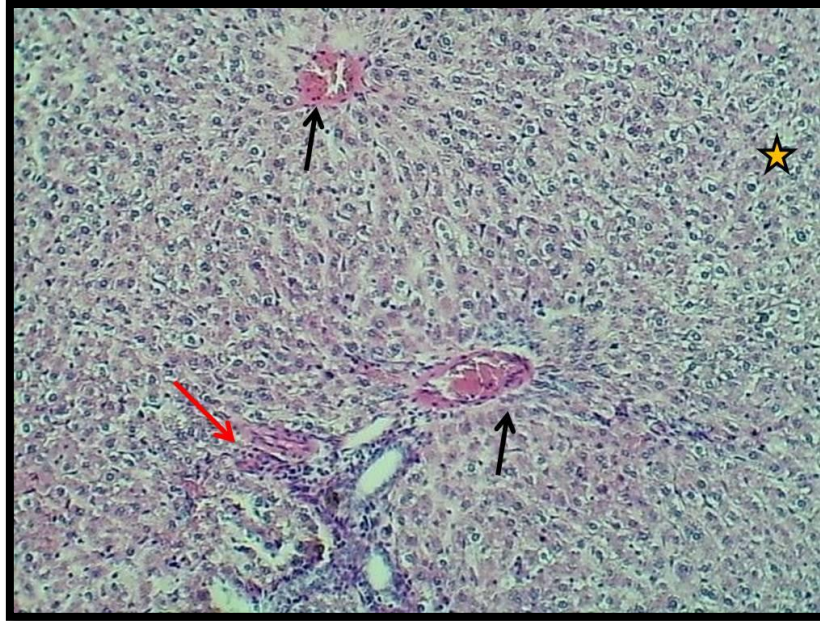


Figure 8. This figure shows vascular congestion (black arrows), pre-vascular infiltration of MNCs (red arrow), and moderate cellular swelling (asterisk). H&E stain 100x.

Histopathological Changes in the Lung

Histopathological figures of the lung showed mild interstitial bronchopneumonia characterized by moderate thickening of interstitial tissue per bronchial infiltration of MNCs and medial thickening of the pulmonary artery with congestion (Fig. 9). Other figures showed severe congestive interstitial pneumonia associated with severe congestion of vascular interstitial tissue and infiltration of MNCs and marked pulmonary emphysema (Fig. 10). Most histopathological figures of the lung showed severe interstitial bronchopneumonia characterized by a damaged lung parenchyma with severe diffused infiltration of MNCs and hyperplasia of bronchial lining cells with marked intra-luminal hemorrhagic (Fig. 11). Other figures showed granulomatous pneumonia, which revealed a marked necrotic center associated with damaged lung tissue, severe infiltration of MNCs, and giant cell formation; there was also bronchial epithelial sloughing (Fig. 12).

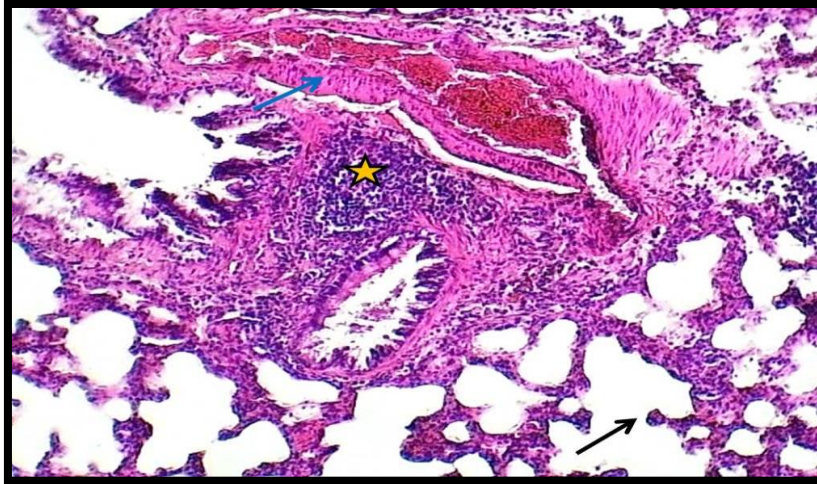


Figure 9. A section of the lung shows mild interstitial bronchopneumonia characterized by moderate thickening of interstitial tissue (black arrow) per bronchial infiltration of MNCs (asterisk), medial thickening of the pulmonary artery (blue arrow), and congestion. H&E stain 10x

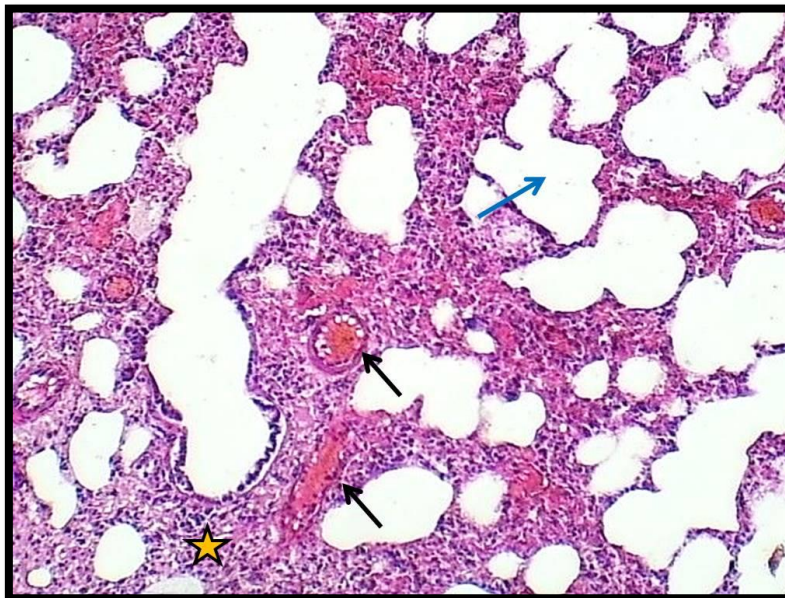


Figure 10. This figure shows severe congestive interstitial pneumonia associated with severe congestion of vascular interstitial tissue and infiltration of MNCs with marked pulmonary emphysema (blue arrow). H&E stain 100x



Figure 11 shows severe interstitial bronchopneumonia characterized by damaged lung parenchyma (asterisks) with diffused infiltration of MNCs (yellow arrow) and moderate hyperplasia of bronchial lining cells with marked intra-luminal hemorrhagic (red arrows). H&E stain 100x.

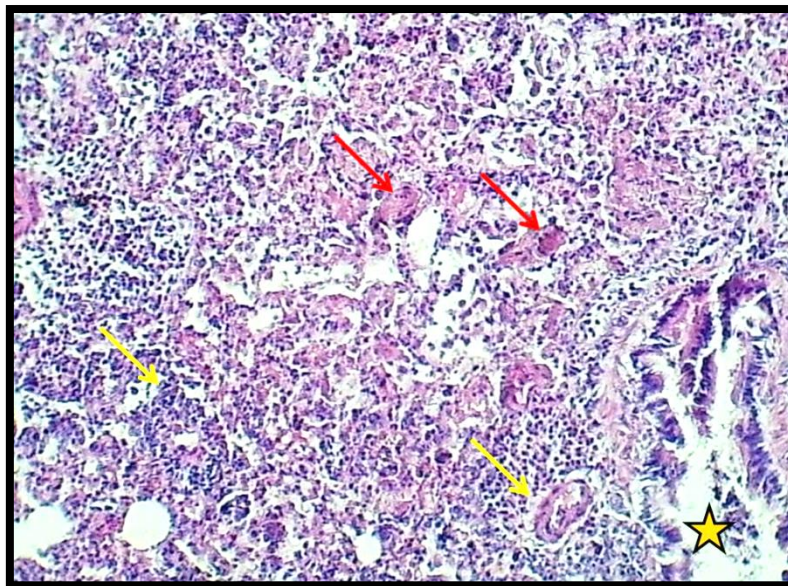


Figure 12. This figure shows a granulomatous lesion that revealed a marked necrotic center with severe infiltration of MNCs (yellow arrows), giant cell formation (red arrows), and bronchial epithelial sloughing (asterisks). H&E stain 40x.

Discussion

Histopathological figures of the liver of all animals revealed marked generalized cellular swelling. It is thought to be produced by membrane damage, which enables fluid to enter the cell, or by cytoskeleton damage, which results in cell shape loss. as mentioned by Shimada et al. (2014). The large quantity of SEB deposited in the liver may be due to SEB absorption by Kupffer cells. SEB has been involved in the pathophysiology of liver damage in experimental hepatitis models (Yang, 2015). Necrosis in the liver is frequently a reaction to extrinsic insults such as drugs, toxins, infection, ischemia, and trauma. Another study showed that the necrosis in the liver caused by SEB occurs in a cascade of events that activate T-cells and kupffer cells; KCS are the primary creators of TNF, which leads to the expansion of necrotic foci (Schümann et al., 2000). which agree with our results. Vasodilation lowers blood pressure by increasing blood flow and reducing systemic vascular resistance (SVR), which are both caused by vasodilation. (hypotension), this finding agrees with our finding about the role of SEB in vasodilation and subsequent hypotension (Purwanasar et al., 2022). The aggregation of MNLs is a result of the movement of leukocytes from the bloodstream to the tissue, which is a pivotal aspect of the inflammatory response. However, these actions seem to happen only after the endothelial cells in the inflamed area have been stimulated by proinflammatory cytokines, such as TNF- α and IL-1 β . In response to such cytokines, ICAM-1, a member of the Ig superfamily, is expressed ubiquitously. ICAM-1 has been found to play a role in leukocyte adhesion to endothelial cells by binding to LFA-1 and Mac-1, its counter-receptors. An increase in ICAM-1 expression has been linked to the accumulation of leukocytes at sites outside of the vasculature in pathological conditions (Tessier et al., 1998). Necrosis may develop as a result of liver injury and inflammation, which cause the release of cytokines like TNF- β and reactive oxygen species (ROS) by hepatocytes and inflammatory cells. These mediators may cause the plasma and mitochondrial membranes to become peroxidized, which ultimately results in either apoptosis or necrosis—two different ways that cells might die (Del Campo et al., 2015). Inflammation causes a stress response in hepatocytes, which can lead to lipid buildup and so may precede steatosis (Tilg and Moschen, 2010). This finding supports our findings. In a separate study, steatosis was discussed in terms of its correlation with VLDL. The study revealed that inhibiting the hepatic secretion of VLDL disrupts the distribution of triglycerides derived from the liver to other bodily

tissues, ultimately leading to the accumulation of triglycerides in the liver. Lowered levels of triglycerides in the bloodstream were observed, while the inhibition of VLDL secretion resulted in hepatic steatosis. This condition was accompanied by heightened levels of ceramides and diacylglycerols within the liver (Minehira et al., 2008). It was discovered in another study that the SEB used in investigation affected the cellular immune response with an increase in leukocytes, lymphocytes, monocytes, and eosinophils on day 6 post-infection (Schümann et al., 2008). Histopathological figures of the liver revealed marked liver cirrhosis that was characterized by thickening of the interlobular connective tissue with marked sinusoidal dilation. Inflammation and T cell activation in cirrhosis are also accompanied by increased anti-inflammatory cytokines, decreased monocyte MHC class II expression, and attenuated cytokine production in T cells, especially elevated serum interleukin-10 levels, which are elevated in patients with cirrhosis (Peter et al., 2013). Numerous reports in the literature indicate that the initiation of an acute inflammatory response in the liver promotes the advancement of liver fibrosis and cirrhosis in patients with steatohepatitis (Del Campo et al., 2018). We conclude from the results that we obtained from the histological sections that the SEB toxin is characterized by a great ability to cause an inflammatory response followed by large, gradual histological changes from cell swelling to liver fibrosis as a result of exposure to the toxin. This is because the toxin used is superantigen, which is characterized by its superior ability to evade the host immune system and cause significant pathological damage.

Our findings are consistent with those of a previous study. The administration of SEB caused the development of interstitial pneumonia as a result of increased mononuclear cell infiltration, which was especially evident around the bronchi and in the peri-arterial area, and an increase in pulmonary interstitial collagen fibers. Another study found that SEB causes interstitial pneumonia by increasing reactive oxygen and nitrogen species, which are also involved in the pathophysiology of lung damage and fibrosis (Shinbori et al., 1996). Congestive interstitial pneumonia is usually the first stage of infection when a pneumonia infection has taken over one of the lungs' lobes. The presence of SEB in the lung leads to inflammation, anoxia, hypotension, and possibly death. SEB causes massive immune cell infiltration into the lung, which is evident by an increase in the number of mononuclear cells overall following SEB exposure, leading to acute inflammatory lung damage. MNC

infiltration occurs around the bronchioles and air vessels; these results were mentioned by Alghetaa et al. (2021). agree with our findings. Exposure to Staphylococcal enterotoxin B (SEB) causes a loss of alveolar capillary membrane integrity, resulting in trans-endothelial immune cell infiltration and the release of various cytotoxic and pro-inflammatory mediators, such as interferons. C (IFN-c), interleukin 6 (IL-6), IL-8, and tumor necrosis factor alpha (TNF-a). Inflammatory activities damage a substantial percentage of sensitive, normal, and compatible lung tissue. This is followed by the formation of pulmonary emphysema, which is characterized by chronic abnormal growth of the air spaces distal to the terminal bronchioles and may also arise as a result of mucus hypersecretion obstruction and subsequent trapping, distension, or destruction of the alveoli. The surrounding bronchus is compressed, increasing airway resistance and the effort required to keep breathing attempts going (Alghetaa et al., 2021). In turn, IL-8 causes tissue damage by stimulating neutrophil infiltration, the release of lysosomal enzymes, and the production of superoxide anions by neutrophils (Sultan et al., 2021). While neutrophils have long been thought to be the primary cause of emphysema, macrophages, T lymphocytes, and eosinophils are now implicated in the pathophysiology of lung deterioration in emphysema (Shinbori et al., 1996). Mesenchymal cell proliferation, elastin and collagen accumulation, and malfunctioning endothelial cells cause bronchial lining epithelial cell hyperplasia. Failure to regulate endothelium-derived mediators, growth factors, and inflammatory processes causes endothelial dysfunction and vascular remodeling (Wells et al., 2015). study showed that seb induces sloughed epithelial cells, lumina contained an exudate composed of similar inflammatory cells, and hemorrhage, which agrees with our finding (Onai and Kudo, 2001). The higher-pressure bronchial system is often the cause of bleeding from the pulmonary or bronchial vasculature. Massive pulmonary bleeding can have a number of common causes, such as lung cancer, lung abscess, pneumonia, chronic bronchitis, and acute bronchitis. A number of causes can produce granulomatous inflammation, including infection, autoimmune disease, toxic, allergic, drug, and neoplastic disorders. Lung granulomas are often generated by a natural bodily process in which the immune system attempts to keep foreign material out of the lungs. It might be a bacterium or toxins (Wilson and Wynn, 2009). Bronchial epithelial sloughing was the result of severe inflammation caused by seb, as found in another study (Krakauer et al., 2009).

Conclusion

The SEB can activate a significant fraction of T lymphocytes. A cytokine storm brought on by such activation causes major damage to interior tissues. We conclude from the results that we obtained from the histological sections that the SEB toxin is characterized by a great ability to cause an inflammatory response followed by large, gradual histological changes from cell swelling to liver fibrosis as a result of exposure to the toxin. This is because the toxin used is superantigen, which is characterized by its superior ability to evade the host immune system and cause significant pathological damage.

References

- Murray, P. R., Rosenthal, K. S., Kobayashi, G. S., & Pfaller, M. A. (1998). Paramyxovirus. *Medical Microbiology, 3rd edition. St. Louis: Mosby*, 461-71.
- Janssen YM, Van Houten B, Borm PJ, Mossman BT. Cell and tissue responses to oxidative damage. *Laboratory investigation; a journal of technical methods and pathology.* 1993 Sep 1;69(3):261-74.
- Madigan, M. T., Martinko, J. M., & Parker, J. (2004). Brock. Biología de los microorganismos.
- Tortora, G. J., Case, C. L., Bair III, W. B., Weber, D., & Funke, B. R. (2004). Microbiology: an introduction. (*No Title*).
- Jardetzky, T. S., Brown, J. H., Gorga, J. C., Stern, L. J., Urban, R. G., Chi, Y. I., ... & Wiley, D. C. (1994). Three-dimensional structure of a human class II histocompatibility molecule complexed with superantigen. *Nature*, 368(6473), 711-718.
- Finegold, M. J. (1967). Interstitial pulmonary edema. An electron microscopic study of the pathology of staphylococcal enterotoxemia in rhesus monkeys. *Lab Invest*, 16(6), 912-924.
- Zhang, P., Yu, J., Gui, Y., Sun, C., & Han, W. (2019). Inhibition of miRNA-222-3p relieves staphylococcal enterotoxin B-induced liver inflammatory injury by upregulating suppressors of cytokine signaling 1. *Yonsei medical journal*, 60(11), 1093-1102.
- Marrack, P. H. I. L. I. P. P. A., Blackman, M., Kushnir, E., & Kappler, J. (1990). The toxicity of staphylococcal enterotoxin B in mice is mediated by T cells. *The Journal of experimental medicine*, 171(2), 455-464.
- Marrack, P., & Kappler, J. (1990). The staphylococcal enterotoxins and their relatives. *Science*, 248(4956), 705-711.
- McKallip, R. J., Do, Y., Fisher, M. T., Robertson, J. L., Nagarkatti, P. S., & Nagarkatti, M. (2002). Role of CD44 in activation-induced cell death: CD44-deficient mice exhibit enhanced T cell response to conventional and superantigens. *International immunology*, 14(9), 1015-1026.
- Rajagopalan, G., Sen, M. M., Singh, M., Murali, N. S., Nath, K. A., Iijima, K., ... & David, C. S. (2006). Intranasal exposure to staphylococcal enterotoxin B elicits an acute systemic inflammatory response. *Shock*, 25(6), 647-656.
- Hayworth, J. L., Mazzuca, D. M., Vareki, S. M., Welch, I., McCormick, J. K., & Haeryfar, S. M. (2012). CD1d-independent activation of mouse and human iNKT cells by bacterial superantigens. *Immunology and cell biology*, 90(7), 699-709.

- Schramm, R., & Thorlacius, H. (2003). Staphylococcal enterotoxin B-induced acute inflammation is inhibited by dexamethasone: important role of CXC chemokines KC and macrophage inflammatory protein 2. *Infection and immunity*, 71(5), 2542-2547.
- Strandberg KL, Rotschafer JH, Vetter SM, Buonpane RA, Kranz DM, Schlievert PM. Staphylococcal superantigens cause lethal pulmonary disease in rabbits. *The Journal of infectious diseases*. 2010 Dec 1;202(11):1690-7.
- McKallip RJ, Fisher M, Do Y, Szakal AK, Gunthert U, Nagarkatti PS, Nagarkatti M. Targeted deletion of CD44v7 exon leads to decreased endothelial cell injury but not tumor cell killing mediated by interleukin-2-activated cytolytic lymphocytes. *Journal of Biological Chemistry*. 2003 Oct 31;278(44):43818-30.
- Uchakina ON, Castillejo CM, Bridges CC, McKallip RJ. The role of hyaluronic acid in SEB-induced acute lung inflammation. *Clinical Immunology*. 2013 Jan 1;146(1):56-69.
- McKallip RJ, Hagele HF, Uchakina ON. Treatment with the hyaluronic acid synthesis inhibitor 4-methylumbelliferone suppresses SEB-induced lung inflammation. *Toxins*. 2013 Oct 17;5(10):1814-26.
- Johnson HM, Torres BA, Soos JM. Superantigens: structure and relevance to human disease. *Proceedings of the Society for Experimental Biology and Medicine*. 1996 Jun;212(2):99-109.
- Schantz, E. J., Roessler, W. G., Wagman, J., Spero, L., Dunnery, D. A., & Bergdoll, M. S. (1965). Purification of staphylococcal enterotoxin B. *Biochemistry*, 4(6), 1011-1016.
- Shimada, M., Cheng, J., & Sanyal, A. (2014). Fatty liver, NASH, and alcoholic liver disease. Yang, Z. (Ed.). (2015). *Chinese burn surgery*. Springer.
- Schumann, J., Wolf, D., Pahl, A., Brune, K., Papadopoulos, T., van Rooijen, N., & Tiegs, G. (2000). Importance of Kupffer cells for T-cell-dependent liver injury in mice. *The American journal of pathology*, 157(5), 1671-1683..
- Purwanasari, H. N., Permatasari, A. T. U., Lestari, F. B., Wasissa, M., Zaini, K., & Salasia, S. I. O. (2022). Cellular immune response of Staphylococcus aureus enterotoxin B in Balb/c mice through intranasal infection. *Veterinary World*, 15(7), 1765.
- Tessier, P. A., Naccache, P. H., Diener, K. R., Gladue, R. P., Neote, K. S., Clark-Lewis, I., & McColl, S. R. (1998). Induction of acute inflammation in vivo by staphylococcal superantigens. II. Critical role for chemokines, ICAM-1, and TNF- α . *The Journal of Immunology*, 161(3), 1204-1211.
- Del Campo, J. A., Gallego, P., & Grande, L. (2018). Role of inflammatory response in liver diseases: Therapeutic strategies. *World journal of hepatology*, 10(1), 1.
- Tilg, H., & Moschen, A. R. (2010). Evolution of inflammation in nonalcoholic fatty liver disease: the multiple parallel hits hypothesis. *Hepatology*, 52(5), 1836-1846.
- Minehira, K., Young, S. G., Villanueva, C. J., Yetukuri, L., Oresic, M., Hellerstein, M. K., ... & Tappy, L. (2008). Blocking VLDL secretion causes hepatic steatosis but does not affect peripheral lipid stores or insulin sensitivity in mice. *Journal of lipid research*, 49(9), 2038-2044.
- Peter, J., Frey, O., Stallmach, A., & Bruns, T. (2013). Attenuated antigen-specific T cell responses in cirrhosis are accompanied by elevated serum interleukin-10 levels and down-regulation of HLA-DR on monocytes. *BMC gastroenterology*, 13, 1-10.
- Del Campo, J. A., Gallego, P., & Grande, L. (2018). Role of inflammatory response in liver diseases: Therapeutic strategies. *World journal of hepatology*, 10(1), 1.

- Shinbori, T., Matsuki, M., Suga, M., Kakimoto, K., & Ando, M. (1996). Induction of interstitial pneumonia in autoimmune mice by intratracheal administration of superantigen staphylococcal enterotoxin B. *Cellular immunology*, 174(2), 129-137.
- Alghetaa, H., Mohammed, A., Zhou, J., Singh, N., Nagarkatti, M., & Nagarkatti, P. (2021). Resveratrol-mediated attenuation of superantigen-driven acute respiratory distress syndrome is mediated by microbiota in the lungs and gut. *Pharmacological research*, 167, 105548.
- Sultan, M., Alghetaa, H., Mohammed, A., Abdulla, O. A., Wisniewski, P. J., Singh, N., ... & Nagarkatti, M. (2021). The endocannabinoid anandamide attenuates acute respiratory distress syndrome by downregulating miRNA that target inflammatory pathways. *Frontiers in Pharmacology*, 12, 644281.
- Wells, J. M., Iyer, A. S., Rahaghi, F. N., Bhatt, S. P., Gupta, H., Denney, T. S., ... & Dransfield, M. T. (2015). Pulmonary artery enlargement is associated with right ventricular dysfunction and loss of blood volume in small pulmonary vessels in chronic obstructive pulmonary disease. *Circulation: Cardiovascular Imaging*, 8(4), e002546.
- Onai, H., & Kudo, S. (2001). Suppression of superantigen-induced lung injury and vasculitis by preadministration of human urinary trypsin inhibitor. *European journal of clinical investigation*, 31(3), 272-280.
- Wilson, M. S., & Wynn, T. A. (2009). Pulmonary fibrosis: pathogenesis, etiology and regulation. *Mucosal immunology*, 2(2), 103-121.
- Krakauer, T., Buckley, M. J., Huzella, L. M., & Alves, D. A. (2009). Critical timing, location and duration of glucocorticoid administration rescue mice from superantigen-induced shock and attenuate lung injury. *International immunopharmacology*, 9(10), 1168-1174.